Welding Institute of Canada
Institut de Soudage du Canada

WELDING INSTITUTE OF CANADA
INSTITUT DE SOUDAGE DU CANADA
HEAD OFFICE: 391 Burnhamthorpe Road East, Oakville, Ont. L6J 6C9 - Ph:(416) 845-9881

STUDY TO IMPROVE SOLIDIFICATION CRACKING RESISTANCE OF SUBMERGED ARC WELD METAL

Welding Institute of Canada Report RC247/3/86

CANMET Contract No. 4-9296

Serial No. OGR84-00323

4/99

Approved by:

Dr. A. G. Glover,
Director of Technology

MICROMEDIA

Prepared by: R. B. Lazor
W. F. Fearis

March 26, 1986

TABLE OF CONTENTS

		Page
	List of Tables	iii
	List of Figures	iv
1.0	Introduction	1
2.0	Theories of Solidification Cracking	2
	2.1 Weld Pool Solidification	2
	2.2 Influence of Composition on Solidification Cracking	4
	2.3 Effect of Oxygen Content on Solidification Cracking	7
	2.4 Effects of Welding Conditions on Hot Cracking	8
	2.5 Ductility of Solidification Structure	8
3.0	Experimental Program	9
	3.1 Baseplate and Consumables	10
	3.2 Transvarestraint Test Results	11
	3.3 Discussion of Results	12
	3.3.1 Weld Pool Chemistry	12
	3.3.2 Transvarestraint Tests	14
	3.3.3 Implication of Results	15
	3.4 Summary	16
4.0	References	17

LIST OF TABLES

		Page
1.	Chemical Composition of Baseplate and Wires	19
2.	Summary of Cracking on Weld Sections	20
3.	Weld Deposit Chemistries	21

LIST OF ILLUSTRATIONS

		Page
1.	Solidification cracks may be observed along the weld centreline, originating from the flare angle, or randomly through the bead.	22
2.	Typical pool shapes revealed by blowout technique for welding speeds of 10, 15, 20, 30, 45, 60 and 74 cm/min.	23
3.	Schematic representation of a weld pool with velocity V.	24
4.	Schematic representation of a teardrop shaped pool.	24
5.	Iron-carbon (Fe-C) equilibrium diagram in the peritectic region.	25
6.	Constitutional diagram of peritectic reaction of Fe-Ni system.	26
7.	Effects of carbon content of weld metal and strength of base metal on the hot cracking.	26
8.	Effect of the oxygen in the weld metal and the heat input on solidification cracking.	27
9.	Ductility curves of different carbon steels.	27
10.	Transvarestraint testplate.	28
11.	Principle of operation of Transvarestraint test.	28
12.	Variation in manganese content versus amperage for welds deposited at 29 V.	29
13.	Variation in manganese content against arc voltage for welds deposited at 550 A.	29
14.	The influence of arc current on the transfer of carbon from the wire to the deposit.	30
15.	Variation in Si content versus current for welds deposited at 29 V.	31
16.	The influence of arc voltage on Si content for welds deposited at 550 A.	31
17.	The influence of current on carbon content at an arc voltage of 29 V.	32

List of Illustrations (Cont'd)

		Page
18.	Variation in carbon content as a function of arc voltage for welds deposited at 550 A.	32
19.	Typical example of solidification cracks observed on cross-section of Transvarestraint specimen.	33
20.	Detail of faces for examination of cracking in Transvarestraint tests.	33
21.	Crack severity versus deflection for Series 1 and Series 6 welds, high C EM12K/LA59.	34
22.	Crack severity versus deflection for Series 2 and Series 7 welds, EM12/LA59.	34
23.	Crack severity versus deflection for Series 3 and Series 8 welds, EM12/LA59 with Si addition.	35
24.	Crack severity versus deflection for Series 4 and Series 9 welds, low C EM12K/LA59.	35
25.	Crack severity versus deflection for Series 5 and Series 10 welds, EH14, 2% Mn/LA589.	36

STUDY TO IMPROVE SOLIDIFICATION CRACKING RESISTANCE OF SUBMERGED ARC WELD METAL

Welding Institute of Canada Report RC247/3/86

1.0 Introduction

The incidence of weld metal solidification cracking, also known as hot cracking, became more prevalent with the advent of high productivity joining processes such as submerged arc welding which is characterized by large weld deposits and coarse columnar structures. The cracks are always intergranular in nature and are classified according to their location in the weld. Centreline cracks, as in Figure 1(a), occur along the centre of the weld, often running their entire length. These cracks are not always observed on the surface of the bead. Flare or butterfly cracks originate from the corner of the weld as shown in Figure 1(b), and are much shorter than centreline cracks. Crater cracks are also quite short and are observed in a semi-circular zone around the weld, see Figure 1(c).

Solidification cracking in submerged arc welding is influenced mainly by composition, and it is particularly pronounced with high levels of impurity elements. Other important factors include the stresses across the joint during the final stages of solidification and the solidification structure of the weld pool.

This study reviews the mechanisms responsible for crack formation, the influence of alloying elements on solidification cracking, and discusses ways in which cracking can be prevented in practice. As an example of an experimental approach used to address solidification cracking, this work also includes results of Transvarestraint tests conducted using several flux/wire combinations recommended for welding low-alloy, C-Mn steels.

2.0 Theories of Solidification Cracking

The susceptibility of weld metals to solidification cracking under given welding conditions and joint geometry depends on the solidification process in the weld pool and the solidification range of the alloy being studied. Weld metals usually solidify in a dendritic mode which promotes solute variations, or microsegregation, within the weld. Solute enrichment leads to regions which have lower melting temperatures than the majority of the pool. These regions of high solute content become trapped between the solidifying cells and dendrites and, when these liquid/solid areas are acted upon by thermal shrinkage strains, they are prone to solidification cracking. The brittle temperature range (BTR) is the range over which cracks will occur. The upper limit of BTR is the temperature at which the flow of liquid between the dendrites is restricted. The lower bound is just below the solidus and is the temperature below which the weld can resist the thermal strains. An increase in solute content due to segregation increases the solidification range, and consequently the susceptibility to solidification cracking is greater.

The various theories proposed to explain the mechanism by which solidification cracks initiate all implicate the composition as having the predominant influence. Researchers argue that either the magnitude of strain across the weld (1) or the strain rate (2) ultimately determines whether or not the weld will be susceptible to solidification cracking. The exact mechanism(s) by which cracks occur will not be considered in detail, attention will focus on composition and the incidence of cracking as related to temperature.

The process of weld pool solidification will be presented so that the following discussions can refer to particular aspects of the solidification of the weld and how they influence cracking.

2.1 Weld Pool Solidification

Weld solidification structures are related to the shape of the weld pool, and they are influenced primarily by the welding speed (3). At slow welding speeds the pool shape is elliptical, while at higher welding speeds the pool

assumes an elongated tear-drop shape. An example of the pool shape progression with changes in welding speed for a given situation is shown in Figure 2. The shape of a weld pool, once established, does not change provided that the welding speed, V, remains constant. The change in weld pool shape with velocity is related to the removal of heat from the weld pool and the consequent solidification characteristics. For the general case of an elliptical weld pool (Figure 3), heat is supplied to the leading edge of the pool, (ABC), while heat must be liberated along the trailing boundary, (CDEA), for solidification to occur. At any point along the solidifying edge of the pool, the growth of the solid occurs parallel to the maximum thermal gradient, meaning that the solid-liquid interface is perpendicular to these gradients. The growth rate, R, at any point along the interface can be related to the velocity, V, and the angle between the average growth direction and the welding direction, ϕ, as given here:

$$R = V \cos \phi \qquad (1)$$

Therefore, the growth rate can be seen to vary from R = 0 at A or C to R = V at the tail of the pool, E.

The growth rate predicted from eq (1) will always be maximized in directions parallel to the welding direction. However, as the velocity increases, the removal of latent heat from the tail of the pool cannot match the required growth rate, and the pool assumes a tear-dropped shape as in Figure 4. These tear-drop shaped pools have straight macroscopic interfaces along much of the solidification boundary, and a small radius of curvature at the tail. This means that growth rate is constant over the straight edges of the pool but that the maximum value of R decreases in accordance with the angle ϕ. The pool shape changes to a more elongated form with increases in welding speed in order to balance the heat flow conditions.

The microsegregation pattern in a weld changes from the fusion boundary to the weld centreline owing to decreases in the ratio of the temperature gradient, G, and the solidification velocity, or growth rate, R. With decreasing values of G/R, solidification theory predicts changes in the microsegregation pattern from planar, through cellular, cellular dendritic, to branched dendritic. Practically speaking, however, solidification microstructures are almost

entirely cellular dendritic, with increased branching towards the centre of the weld, attributable to the decrease in the G/R ratio.

The sensitivity to hot cracking is related to the shape of the weld pool. Elliptical weld pools are moderately insensitive to centreline hot cracking while teardrop shaped pools are particularly sensitive to the problem. This results because of the impingement of two solid/liquid dendritic interfaces of high solute content along the weld centreline.

2.2 Influence of Composition on Solidification Cracking

The level(s) of impurity elements and the overall alloy content are extremely important in determining the susceptibility to cracking. Segregation of impurity elements such as phosphorous and sulphur to the weld centreline promotes the formation of low melting temperature solids and increases the risk of cracking. The degree of segregation depends on the solubilities of these elements in the advancing solid. Austenite has a very low solubility for both sulphur and phosphorous, whereas delta-ferrite has a greater solubility for both of these elements. Another explanation for reduced cracking is that the liquid phases are dispersed through distribution of the delta-ferrite (17). Therefore, alloys solidifying by delta-ferrite would have a lower risk to solidification cracking than those which solidify as austenite. The overall composition determines the nature of solidification, being either austenite or delta-ferrite, Figure 5. In steels with carbon contents above 0.15 percent, solidification proceeds by the formation of austenite. Below 0.10 percent carbon, solidification occurs to the left of the peritectic point by the formation of delta-ferrite. Austenite-stabilizing elements such as carbon, manganese, copper, and nickel, which shift the peritectic reaction to the left, promote solidification by austenite, and the resultant segregation can lead to solidification cracking. Although Mn promotes cracking by stabilizing austenite, it is beneficial from the point of view of its interaction with sulphur (9). Depending on the C content, a minimum Mn/S ratio can prevent hot cracking. The benefit of increased Mn is that it ties up sulphur as MnS inclusions, thus preventing the formation of FeS films along grain boundaries; these films have been known to cause cracking. The amount of Mn remaining

in solid solution would then have very little effect on hardenability.

The significance of the peritectic reaction on segregation of phosphorous and sulphur in the Fe-Ni and Fe-C systems, and their influence on hot cracking, was studied by Masumoto and Imai (5) for both SAW and GMAW. Electron probe microanalysis showed sulphur segregation at cracks which coincided with grain boundaries. The sulphur segregation was related to the diagram shown in Figure 6. The observed sulphur concentrations show that the ratio is 1 for delta-ferrite solidification, 8 to 10 in the peritectic range, and up to 20 for solidification as austenite. Weld metals A, B, and C, which did not exhibit segregation, solidified as delta ferrite while E, F, and G solidified through the peritectic reaction. The solubilities of sulphur and phosphorous in delta ferrite are respectively 0.18 and 2.8 percent, compared to 0.05 and 0.3 percent for austenite. Since these impurities have high solubilities in delta-ferrite, solidification through only delta-ferrite may not promote segregation. On the other hand, the low solubilities in austenite will promote segregation to grain boundaries.

The hot cracking sensitivity of the weld for increasing carbon contents was shown (5) to behave in a similar manner to nickel, as in Figure 7. Their results show a critical carbon content for cracking of 0.10 percent, which just corresponds to the maximum carbon solubility of delta-ferrite. For a weld metal containing 0.08 percent carbon and 0.027 percent sulphur, no microsegregation was observed, while sulphur segregation was observed at a crack in weld metal with 0.14 percent carbon, in spite of a lower sulphur content of 0.01 percent. Finally in Figure 7, it is noted that crater cracks form at lower carbon contents than complete longitudinal cracks. In certain instances, solidification cracking can actually increase with lower carbon contents. Ohshita and his co-workers (6) showed that the critical carbon content ranged from 0.05 to 0.10 percent, with cracks forming in the leaner compositions above a critical travel speed when the weld pool exhibited a dendritic centreline structure.

The increased crack susceptibility with delta-ferrite solidification was attributed to a combination of thermal shrinkage and the shrinkage of the

delta-ferrite to austenite transformation during cooling (6). It is most likely, however, that the morphology of the dendritic centreline structure and the resultant segregation were a greater factor than the transformation strain.

The progression of solidification structures from axial, at slow welding speeds, to equiaxed dendritic, at high welding speeds, has been shown to depend on the microalloy content of the weld metal (7). With small additions of Ti, Nb, and Zr, the welding speeds for the formation of a given macrostructure were suppressed. For the case of equiaxed dendrites, the critical welding speed was lowered by 10 to 20 cm/min, or 14 to 29 percent. This shift was attributed to the heterogeneous nucleation from carbides and nitrides of Ti, Nb and Zr in the molten pool. Nucleation is easiest on TiN and TiC due to the small difference in lattice parameter compared to delta ferrite. The overall effect of the microalloys was to increase the equiaxed zone along the weld centreline. Increasing the carbon content from 0.18 to 0.35 percent was also observed to promote a central equiaxed zone. They provided the explanation that the temperature difference between the liquidus and solidus was greater at higher carbon contents, and consequently, heterogeneous nucleation would occur more easily.

In weld metals, silicon is deliberately added to deoxidize the weld pool, and the final level of Si is often greater than that of the baseplate. The Fe-Si phase equilibrium predicts a peritectic reaction at 1275°C, which means that it is entirely possible to have a low melting temperature solute once the weld has solidified around 1400°C. The occurrence of this peritectic reaction is thought to increase the likelihood of solidification cracking, especially with high Si levels in the weld pool.

Several empirical formulae have been proposed to calculate parameters which describe an effect of alloying elements on solidification cracking. Garland and Bailey (16) used multiple regression analysis to express susceptibility to solidification cracking, in Units of Crack Susceptibility (UCS), based on weld metal composition as follows:

$$UCS = 223\ C + 197\ S + 100\ P + 48\ Nb - 14.3\ Si - 6\ Mn - 16\ Al + 0.5$$

This equation is considered to be valid only for alumina-based neutral fluxes and predicts cracking at UCS values greater than 20. Another expression, developed by Wilkinson (18), uses hot cracking severity (HCS) to rank various alloys:

$$HCS = \frac{C\ (S + P + Si/25 + Ni/100)}{3\ Mn + Cr + Mo + V} \times 103$$

Solidification cracking is likely when HCS exceeds 4.

The papers discussed above showed the significance of the peritectic reaction and the presence of impurity elements on the susceptibility of submerged arc welds to solidification cracking. These factors are both related to the composition of the weld and are determined primarily from the compositions of the baseplate and filler wire. It is also known that the flux itself can influence the chemical composition, as discussed in the following section.

2.3 Effect of Oxygen Content on Solidification Cracking

It has recently been suggested that the weld metal oxygen content is important in relation to solidification cracking. This is because oxide inclusions can mix and incorporate sulphide compounds to form inclusions which are usually spherical, or in some cases, oxisulphide compounds may be formed. This, in effect, stabilizes the sulphur compounds and prevents the formation of films. From this argument, it can be suggested that weld metals of high oxygen content are less susceptible to hot cracking, since there is a higher chance of the sulphides being absorbed into inclusions (11). The inclusion volume fraction is directly related to the oxygen content of the weld, which in turn is determined by the flux type.

Low oxygen levels in submerged arc welding are obtained using basic fluxes, with resultant oxygen levels being around 300 ppm. High oxygen levels (>660 ppm) result from the use of acidic fluxes. Hirabayashi et al (11) have shown, however, that welds with oxygen less than 350 ppm are very susceptible to cracking, while those with greater than 500 ppm oxygen exhibit a low susceptibility to cracking (see Figure 8). From their results one can conclude that acidic fluxes are necessary to prevent solidification cracking.

2.4 Effects of Welding Conditions on Hot Cracking

It has been stated several times that the solidification structure is influenced by the heat input and in turn affects the cracking tendency. The selection of arc voltage and current, travel speed, and wire and flux combination influences the weld metal composition and pool shape.

Arc voltage and current are the parameters which have the greatest impact on solidification cracking through their influence on weld bead shape. High currents and/or low voltages tend to produce deep, narrow welds which exhibit distinct columnar growth from the sides of the pool which is very prone to solidification cracking. Another consequence of deep penetration is that the weld pool contains a greater percentage of baseplate, or greater dilution. When the baseplate has a higher alloy content than the wire, the weld pool will thus have a higher alloy content and could therefore be more susceptible to cracking.

Weld travel speed, by itself, can be lowered to reduce the risk of cracking but economy dictates that high welding speeds should be used whenever possible and therefore other variables are often addressed to reduce cracking.

Bead profile changes (as a function of amperage and voltage) have been used as a means to prevent solidification cracking but are not always realistic in production situations. To maintain high efficiency with a low chance of solidification cracking, Hirabayashi et al (11) employed a high current GMAW + 2 SAW procedure. This approach was effective because the two heat inputs could be separated and the resultant weld pool shape was not susceptible to cracking.

2.5 Ductility of Solidification Structure

In a study of the details of solidification and associated cracking, Matsuda et al (12) were able to show that neighbouring cellular dendrites contact each other at an early stage of solidification, and that cracking initiates at

relatively high temperatures in what has been termed the brittle temperature range (BTR). By direct observation of the cracking event, they were able to calculate the minimum ductility for crack initiation and the BTR.

The ductility of various steels in relation to the carbon content has been determined by Matsuda et al (12) and shown in Figure 9. The temperature of min lies at the high temperature end of the BTR except for the 0.16% steel. These curves suggest that solidification cracking occurs at higher temperatures within the BTR which is in contradiction to previous results (13). Matsuda et al (12) estimated from their fractographic study that liquid droplets exist near the solidus temperature rather than a liquid film and is thereby more crack resistant. This region of min corresponds approximately to the time when neighbouring dendrites rapidly develop to contact each other near the liquidus temperature.

The temperature limits of the BTR and the shape of the ductility curve and its minimum value in the high temperature region depend on the chemical composition of the weld metal. The susceptibility to solidification cracking is increased by raising the temperature interval and decreasing the minimum ductility. It was found (14) that the temperature difference in the BTR is almost in proportion to the normal solidification temperature difference of the alloy. Senda et al (14) also showed that the properties of the ductility curves are not affected by changes in welding variables. However, using the augmented strain test they did show an increase with cracking as current increased. An interesting result from their work showed that cracking was not affected by welding speed. This was attributed to heat flow characteristics which relate the BTR to voltage, current, and efficiency of the heat source only.

3.0 Experimental Program

From the previous discussions the higher than expected incidence of solidification cracking in the submerged arc weld metal appears to be associated with one or more of the following:

1. Chemical composition of the weld pool.

2. Weld pool solidification structure.
3. Basic fluxes.

Although there is general agreement that composition is important, there are several conflicting explanations on how the alloying elements affect cracking. The objectives of this study were to produce welds both with, and without solidification cracks, for several different compositions, and to compare the incidence of cracking for the different welds. The results were expected to suggest which flux/wire compositions are required for toughness and strength requirements with minimum incidence of cracking. Specifically some of the questions to be addressed include:

1. What are the limits on the chemical composition of the weld pool to prevent solidification cracking when using basic fluxes?

2. Does the manner in which silicon is added to the weld, being either in the wire or by additions in the flux, change the susceptibility of the weld to solidification cracking?

3. Is the susceptibility of a given weld deposit greater at low, as opposed to high oxygen contents?

The Transvarestraint test was used for assessing solidification cracking susceptibility. Details of the testplate and the test assembly are shown in Figures 10 and 11. At a predetermined point during welding, the specimen is bent over a former and induces a strain on the top surface to simulate the thermally-induced strains which occur during weld pool solidification.

3.1 Baseplate and Consumables

Two 16 mm thick baseplates were used for the Transvarestraint tests, a 0.20% carbon steel and a 0.07% carbon steel, the compositions of which are listed in Table 1.

Five different flux/wire combinations were chosen, as summarized below:

Series	Flux	Wire
1	LA59	high C EM12K
2	LA59	EM12
3	LA59 with Si addition	EM12
4	LA59	low C EM12K
5	LA589	EH14, 2%Mn

The chemistries of the wire compositions are also listed in Table 1. The main differences in the wires are in the carbon, silicon, and manganese contents. The final weld composition is determined from the interaction between the wire, flux, and the baseplate. The chemical compositions of undiluted weld metals were determined using standard weld pads at several combinations of voltage and current. These results, plotted in Figures 12 to 18, show the changes in carbon, manganese, and silicon in the weld metal with variations in voltage, current, and wire carbon content.

3.2 Transvarestraint Test Results

The Transvarestraint tests were conducted using the single heat input listed below:

Welding Conditions	
Current	500 A
Volts	31 V
Travel speed	400 mm/min
Nozzle to plate distance	25 mm
Energy input	2.3 kJ/mm

This combination of welding parameters produced a bead which just filled the groove shown in Figure 10. Run-on and run-off tabs are used to ensure that welding conditions were stable at the instant of strain application. The deflection was measured 130 mm from the weld centreline and controlled using stops under the test plate. The deflection rate of the specimen was 10.2

mm/s, and was controlled using a dedicated hydraulic system. Welds were deposited using the five flux/wire combinations on both testplates at several different ram deflections. As a minimum, deflections of 0.5 and 1.0 mm were employed.

Crack assessment was conducted using two methods. The first was visual examination of the weld surface using a stereo microscope. Although this has the advantage of providing a fast method for determining the extent of cracking, most solidification cracks are sub-surface and cannot be accounted by this method (see Figure 19). Visual examination was done primarily to help in deciding at which deflections the remaining tests would be conducted.

The extent of cracking was determined using the metallographic technique on polished and etched cross-sections as shown in Figure 20. This technique has been shown to be a preferred method for characterizing the cracking results (19).

The results of the Transvarestraint tests are summarized in Table 2 and plotted in Figures 21, 22, 23, 24 and 25. Each of the figures compare the same flux/wire combination for the two steels. In all cases, the 0.20 percent carbon baseplate exhibits a much greater susceptibility to solidification cracking.

The weld metal compositions of the test welds are listed in Table 3, and they include the weld metal oxygen content. These correlate well with the distribution of non-metallic inclusions in each of the weld series was measured by point counting unetched samples at X1000 magnification (20). Nine fields for each sample were viewed and inclusions were sized in four ranges.

3.3 Discussion of Results

3.3.1 Weld Pool Chemistry

The influence of welding parameters on the undiluted weld pool chemistries is shown in Figures 12 to 18 for manganese, silicon, and carbon. For the case

of manganese, Figures 12 and 13 show that the manganese decreases with increasing current or decreasing voltage, except for the high manganese EH14 wire. In the latter case, the manganese content is shown to be unaffected by either the voltage or current. The silicon content of the weld is affected much more by the current (at a fixed voltage), Figure 15, then by voltage (at a fixed current), Figure 16, over the operating range of the 3.2 mm wires. The EH14 wire exhibited the smallest changes in silicon, while the LA59 flux with added silicon had the largest variations in silicon. The significance of adding silicon through the wire or from the flux is also evident. At 29 V, Figure 15 shows the weld pool silicon content of the LA59/EM12K combination to be similar to the LA59 with Si/EM12 flux and wire combination. At lower currents, however, the LA59 flux with added silicon delivers much more of this element to the pool than the EM12K wire. Similarly, at a fixed current (Figure 16), the silicon content is identical at low voltages, but at higher voltages the LA59 with silicon flux results in more silicon in the weld. These results illustrate that the silicon content of the weld is influenced by the method of silicon addition, the silicon added through the flux is much more effective at low currents and high voltages. In Figure 14, one sees that the carbon content of the deposit increases directly with the wire carbon content, and that the deposit carbon level is higher for the same wire at higher currents. This figure also shows that silicon added to the flux can 'protect' the carbon in the molten weld pool, and can cause the carbon to be higher by as much as 0.005 percent. Increasing the welding current, at fixed voltage, can also give higher weld pool carbon levels (Figure 17), while for the most part, increasing the voltage, at fixed current, does not markedly change the carbon content (Figure 18). In summary, the results show that the weld pool chemistry is influenced by the following:

a) increasing the welding current decreases the manganese (except for EH14) and silicon, while increasing the carbon content,

b) increasing the arc voltage increases the manganese (except for EH14) and silicon contents, while having little influence on the carbon level in the weld pool, and

c) silicon added to the flux will increase the carbon content of the weld.

3.3.2 Transvarestraint Tests

The Transvarestraint tests compare the influence of the weld pool chemistry on the susceptibility to solidification cracking. The results in Figures 21 to 25 clearly show that the high C (0.20) baseplate results in a marked increased in the crack susceptibility compared to the low C (0.07) baseplate. In the latter case, the total crack length did not exceed 6 mm for deflections up to 1.0 mm, while the high C baseplate produced weld metal cracking as high as 31.4 mm.

The low C welds, series 6 to 10, were very similar in cracking behaviour, with only series 6 showing a slightly higher susceptibility to cracking. Series 6 welds were deposited using the LA59 flux and high C, EM12K wire. Small cracks were noted for the other welds up to 1 mm deflection in the low C group, usually less than 3 mm. There was, however, over 5 mm of cracks for series 9, the LA59/Low C EM12K combination, indicating that its composition could be susceptible to cracking.

In the high C baseplate welds of series 1 to 5, the cracking results appear to be in two groups, series 1, 3, and 4, and series 2 and 5. The former group, 1, 3, and 4, had similar compositions, including oxygen contents. Compared to this group weld 2 had higher manganese and oxygen, while weld 5 had a much lower silicon content. These results suggest that the susceptibility to solidification cracking is influenced by a combination of the oxygen and silicon content of the weld pool, and their influence on the deoxidation of the weld pool and/or interdendritic segregation (8). High oxygen levels combine the sulphur as inclusions and thus prevent the formation of interdendritic films. The low susceptibility of series 5 welds, even with a low silicon content, is considered to be due to the high manganese content of the consumable leading to a reaction with the sulphur. The low weld manganese level indicates that the MnS must have combined with the slag, resulting in a low manganese content in the weld.

Comparison of the susceptibilities on the basis of composition using UCS (Table 3) does not differentiate the small differences in susceptibility within

either the low or high carbon groups. The high carbon welds exhibit UCS values averaging about 20, which is the crack/no crack threshold, while series 6 to 10 (low carbon) have UCS values between 7 and 11, indicating a low susceptibility to solidification cracking. In the case of the HCS parameter, none of the deposits were close to the HCS = 4 crack/no crack boundary, but the HCS values did represent the ranking of the deposits within each carbon group (ie welds 1, 3 and 4, and 6, 8, and 9, as predicted by the HCS values in Table 3, had the greatest amount of cracking).

The higher oxygen levels within each carbon group of series 2 and 7 deposits exhibited the lowest susceptibility to solidification cracking. The oxygen level by itself, however, does not determine the susceptibility, since the low carbon group has the lower oxygen content for the same flux/wire combination. The high silicon of the low carbon baseplate (0.19% Si) compared to the baseplate for series 1 to 5 welds (0.02% Si), deoxidizes the pool much more effectively and leads to a lower oxygen content. Since carbon has a greater influence on cracking, it overrides the consequence of lower oxygen in the deposit.

3.3.3 Implication of Results

The occurrence of solidification cracks has been shown to be influenced primarily by the composition of the weld, which in turn is determined by the amount of dilution of baseplate into the weld area. By conducting Transvarestraint tests, one can rapidly determine whether or not a particular flux/wire combination will produce crack-free welds for a given baseplate. If cracks do occur, there are several possible solutions that can be implemented. With reference to the weld pool chemistry results shown in Figures 12 through 18, it is possible to change the chemistry of the weld to attain a crack-free composition. This can be done by changing the welding parameters for the same consumables when only a small change in composition is necessary. When a large shift in composition is required, it most likely would be necessary to change the flux/wire combination and the welding parameters as well. The shifts in composition would also depend on the joint configuration and the amount of dilution. Area measurements of trial welds

will allow one to calculate the dilution and then, combined with the undiluted weld and baseplate compositions, the resultant weld chemistry can be predicted.

It should be remembered that any changes in welding parameters will also produce different depth-to-width ratios of the weld. As has been shown, these are also very important in preventing solidification cracks and it is possible that they can even override the composition effects.

What has been shown, therefore, is a way in which susceptibility to solidification cracking can be assessed and the steps that can be taken to produce crack-free welds on the basis of weld chemistry and welding parameters.

3.4 Summary

The results of the Transvarestraint tests have shown there to be a difference in the susceptibility to solidification cracking as influenced by the weld pool composition. For the tests completed in this project, there was a noticeable effect due to carbon and, to a lesser extent, oxygen. Cracking increases with higher carbon and/or lower oxygen contents. Comparison of the LA59/EM12K and LA59 with silicon/EM12 flux/wire combinations indicated that there was little difference in the crack susceptibilities. This indicates that solidification cracking is not a function of whether the silicon is added through the flux or through the wire.

Within the limited number of tests conducted, it was possible to observe the influence of composition on the tendency to produce solidification cracks. The test can be used to compare baseplate/weld metal combinations for rapid selection of compositions and welding parameters to prevent cracks, particularly in the critical root region in which the weld has a high dilution from the baseplate.

4.0 References

1. J. C. Borland, British Welding Journal, 1960, 7, p 508.

2. N. N. Prokhorov, Welding Production, 1962, 9, p1.

3. T. Ganaha and H. W. Kerr, "TIG Weld Solidification Structures in Carbon Sheet Steels", Metals Technology, Feb 1978, p 62.

4. W. F. Savage, "Solidification, Segregation, and Weld Imperfections", Welding in the World, Vol 18 (5/6), 1980, p 89.

5. I. Masumoto and K. Imai, "A Metallurgical Aspect of Hot Cracking and Toughness of Weld Metal", IIW Doc IX-687-70.

6. N. Yurioka, S. Ohshita, S. Saito and H. Sakurai, "Solidification Cracking Prevention in Pipeline Girth Welding of Low Carbon Steel", Welding In Energy-Related Projects (Toronto: Pergamon Press Canada Ltd, 1984), p 53.

7. K. Nishio, J. Tokunaga, M. Katoh, and S. Mukae, "Effects of Welding Speed and Micro-alloy Element on the Weld Solidification Structures of Steels", Transactions of the Japan Welding Society, Vol 12 (2), 1981, p 34.

8. M. Simpson and W. P. Tait, "Solidification Cracking During the Submerged Arc Welding of Carbon Manganese Steels - A Review", Welding Research International, Vol 7(3), 1977, p 177.

9. P. W. Jones, "An Investigation of Hot Cracking in Low Alloy Steel Welds", British Welding Journal, Vol 6(6), 1959, p 282.

10. T. Wada, as referenced by Ohshita et al (6).

11. K. Hirabayashi, K. Akao, T. Taira and H. Ichinose, "Effect of the Chemical Composition and Welding Method on Hot Cracking", proc Fundamental and Practical Approaches to the Reliability of Welded Structures, Osaka, November 1982, Japan Welding Society, p 383.

12. F. Matsuda, H. Nakagawa, Y. Honda and K. Sorada, "Direct Observation of Solidification and Solidification Cracking During GTA Welding", ibid, p 389.

13. N. N. Prokhorov and N. Nikol Prokhorov, "Fundamentals of the Theory for Technological Strength of Metals While Crystallizing During Welding", Transactions of the Japan Welding Society, Vol 2(2), 1971, p 109.

14. T. Senda, F. Matsuda, G. Takano, K. Watanabe, T. Kobayashi and T. Matsuzawa, "Fundamental Investigations on Solidification Crack Susceptibility for Weld Metals with Trans-Varestraint Test", Transactions of the Japan Welding Society, Vol 2(2), 1971, p 45.

15. W. K. B. Marshall, "A Note on the Relationship Between Chemical Composition and Hot Cracking in Mild and Low Alloy Steels", British Welding Journal, Vol 7(7), 1960, p 451.

16. J. G. Garland and N. Bailey, "Solidification Cracking During Submerged Arc Welding of Carbon-Manganese Steels - A Detailed Assessment of the Effect of Parent Plate Composition", Welding Research International, Vol 8(3), 1978, p 240.

17. N. Yurioka, M. Koike, N. Mori, K. Nagano, "Impact of Welding Research on Steel Composition Development", IIW Doc IX-1313-84.

18. F. J. Wilkinson, British Welding Journal, Vol 5, 1958, p 557.

19. B. F. Dixon, R. H. Philips, and J. C. Ritter, "Cracking in the Transvarestraint Test - Part 1 A New Procedure for Assessment of Cracking", Metal Construction, Vol 16 (2), 1984, p 86.

20. E. Scheil, Z. Anorg, Allgem. Chem., 1931, 201, p 259.

TABLE 1

Chemical Composition of Baseplate and Wires

	C	Mn	S	P	Si	V
247-1	0.20	1.27	0.030	0.008	0.02	0.039
247-2	0.07	1.49	0.003	0.013	0.19	0.07
EM12	0.09	0.95			0.03	
EM12K High C	0.13	0.94	0.017	0.014	0.23	
EM12K Low C	0.11	0.95	0.016	0.013	0.21	
EH14	0.12	1.85			0.05	

TABLE 2

Summary of Cracking on Weld Sections

Steel	Series	Wire/Flux	Deflection mm	Total Crack Lengths, mm on surface 8 Faces mm		Weld Metal Dilution, %
247-1	1	High C EM12K/LA59	0	Nil	0	
			0.5	2.75	17.8	61
			1.0	6.0	31.4	
			3.0	32.0	48.3	
			5.0	32.5	53.3	
	2	EM12/LA59	0	Nil	-	
			0.5	8.5	19.4	68
			1.0	4.5	15.2	
			3.0	22.0	34.2	
	3	EM12/LA59 with Si	0	Nil	-	
			0.5	7.5	29.4	69
			1.0	6.5	20.8	
	4	Low C EM12K/LA59	0	Nil	-	
			0.5	7.5	29.7	69
			1.0	9.0	22.1	
			3.0	12.5	47.8	
	5	EH14/LA589	0	Nil	-	
			0.5	8.3	21.8	67
			1.0	27.5	18.2	
			3.0	35.0	35.6	
247-2	6	High C EM12K/LA59	0.5	2.0	6.3	67
			1.0	Nil	13.3	
			3.0	4.5	18.6	
	7	EM12/LA59	0.5	2.0	2.5	70
			1.0	Nil	2.57	
	8	EM12/LA59 with Si	0.5	Nil	1.5	66
			1.0	Nil	1.14	
	9	Low C EM12K/LA59	0.5	Nil	5.4	65
			1.0	3.0	1.14	
	10	EH14/LA589	0.5	Nil	0.71	65
			1.0	Nil	1.14	

TABLE 3

Weld Deposit Chemistries

Series	C	Mn	S	P	Si	O	UCS(a)	Mn/S	HCS(b)
1	0.11	1.35	0.016	0.013	0.26	221	18.73	84.4	1.07
2	0.12	1.50	0.016	0.013	0.25	342	20.34	93.8	0.953
3	0.11	1.30	0.015	0.013	0.21	281	19.42	86.7	0.971
4	0.12	1.31	0.016	0.011	0.20	219	21.83	81.9	1.07
5	0.11	1.34	0.015	0.011	0.14	245	19.92	89.3	0.865
6	0.09	1.46	0.007	0.016	0.34	174	10.17	208.6	0.752
7	0.08	1.41	0.007	0.016	0.27	289	9.00	201.4	0.639
8	0.08	1.46	0.007	0.016	0.36	255	7.62	208.6	0.683
9	0.08	1.45	0.007	0.015	0.34	202	7.85	207.1	0.673
10	0.08	1.48	0.007	0.015	0.25	222	8.79	211.4	0.577

a) UCS = 230 C + 190 S + 75 P + 45 Nb - 12.3 Si - 5.4 Mn - 1

b) see page 7.

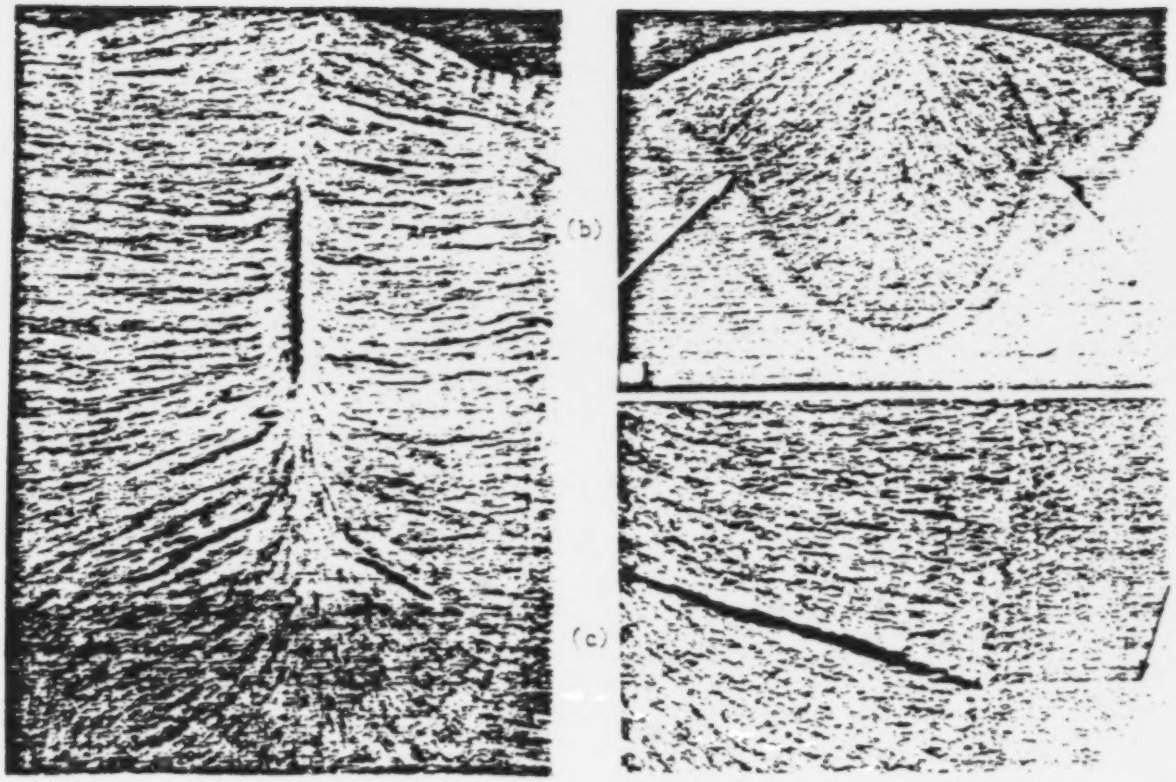

Figure 1. Solidification cracks may be observed, (a) along the weld centreline, (b) originating from the flare angle, or (c) randomly through the bead.

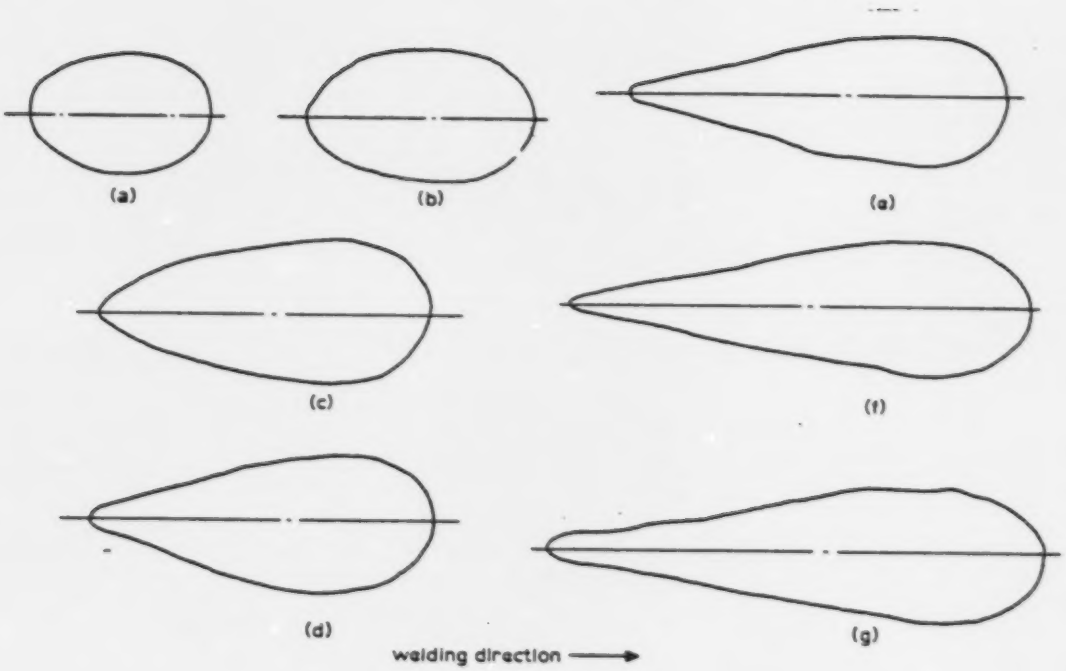

Figure 2. Typical pool shapes revealed by blowout technique for welding speeds of (a) 10 cm/min, (b) 15 cm/min, (c) 20 cm/min, (d) 30 cm/min, (e) 45 cm/min, (f) 60 cm/min, and (g) 74 cm/min, from ref (3).

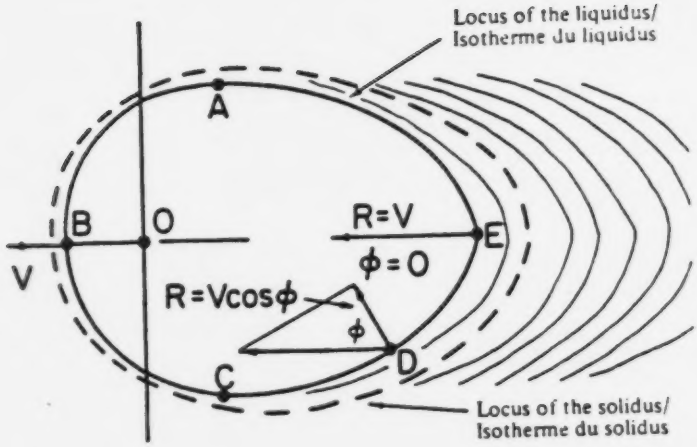

Figure 3. Schematic representation of a weld pool with velocity V. The growth rate, R, varies from R = V at E to R = O at points A and C, ref (4).

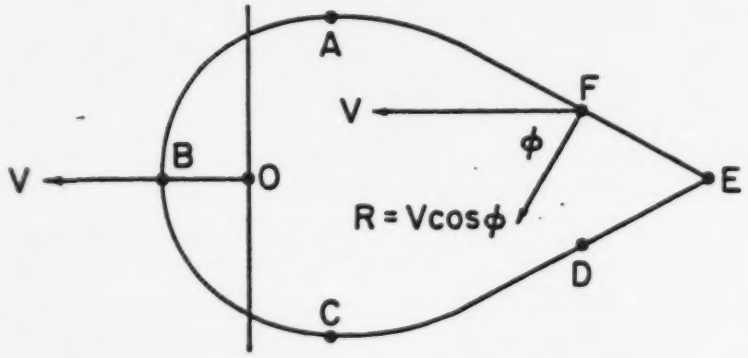

Figure 4. Schematic representation of a teardrop shaped pool, ref (4).

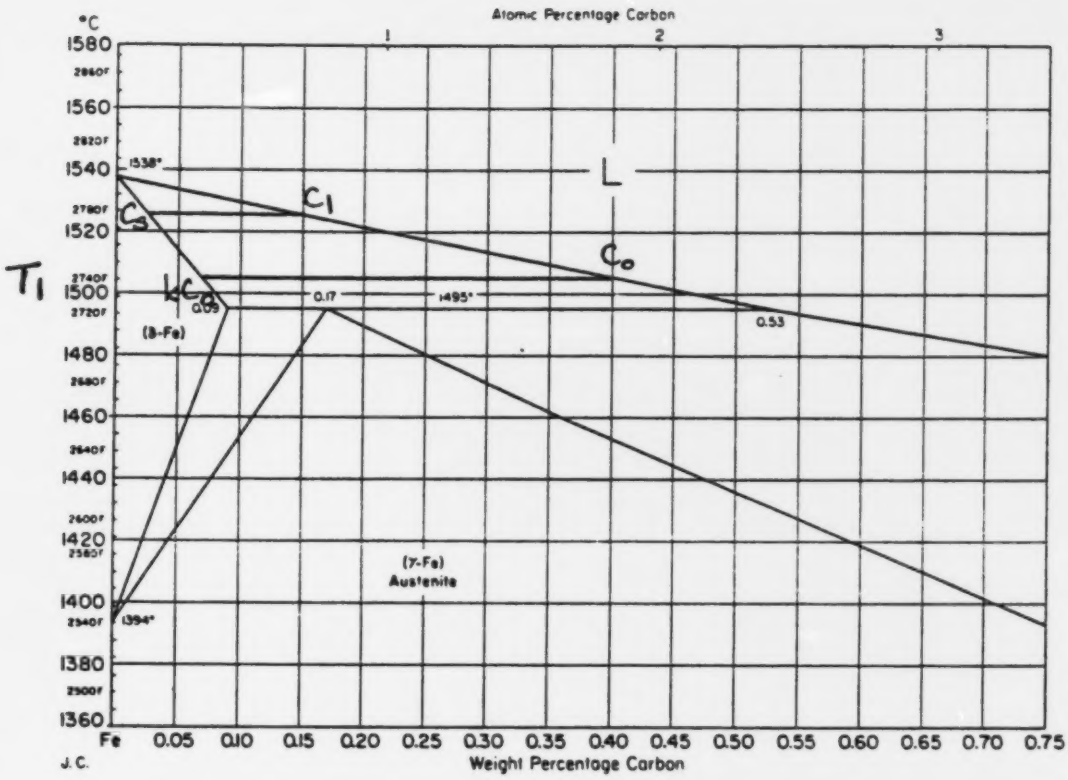

Figure 5. Iron-carbon (Fe-C) equilibrium diagram in the peritectic region.

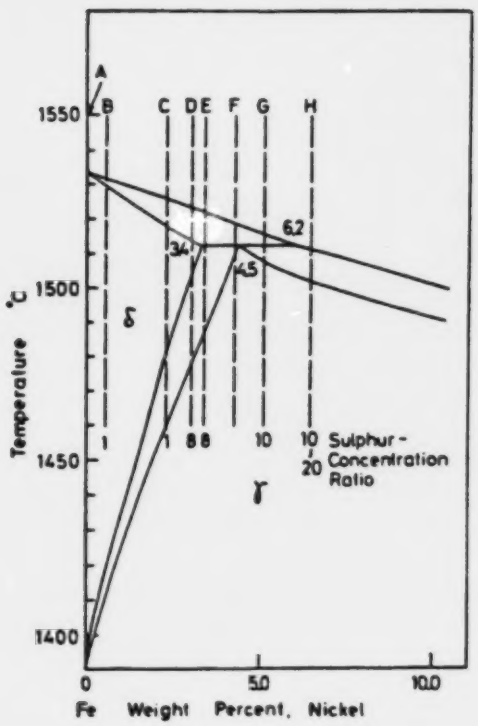

Figure 6. Constitutional diagram of peritectic reaction of Fe-Ni system, ref (5).

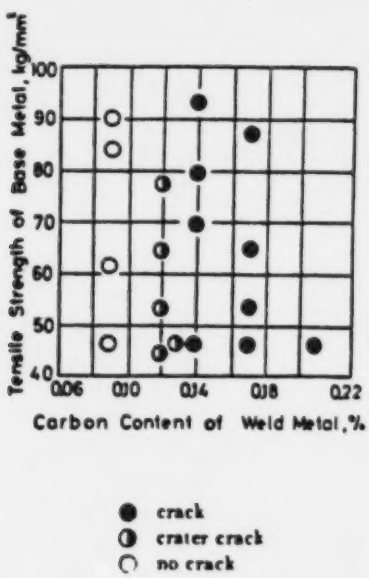

Figure 7. Effects of carbon content of weld metal and strength of base metal on the hot cracking, ref (5).

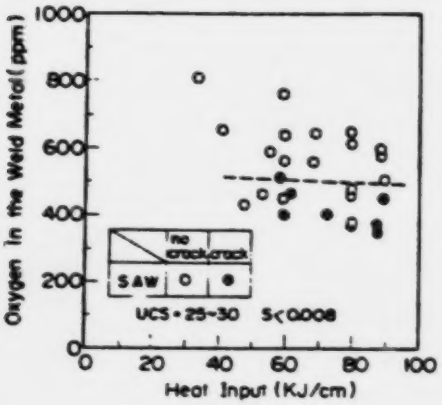

Figure 8. Effect of the oxygen in the weld metal and the heat input on solidification cracking, ref (11).

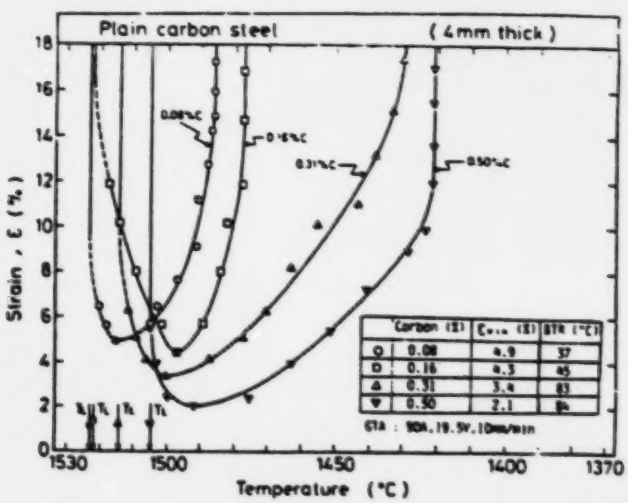

Figure 9. Ductility curves of different carbon steels, ref (12).

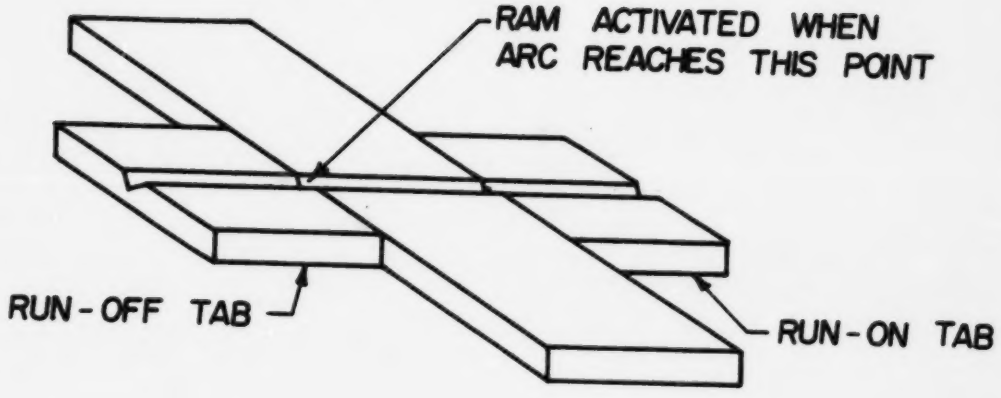

Figure 10. Transvarestraint testplate.

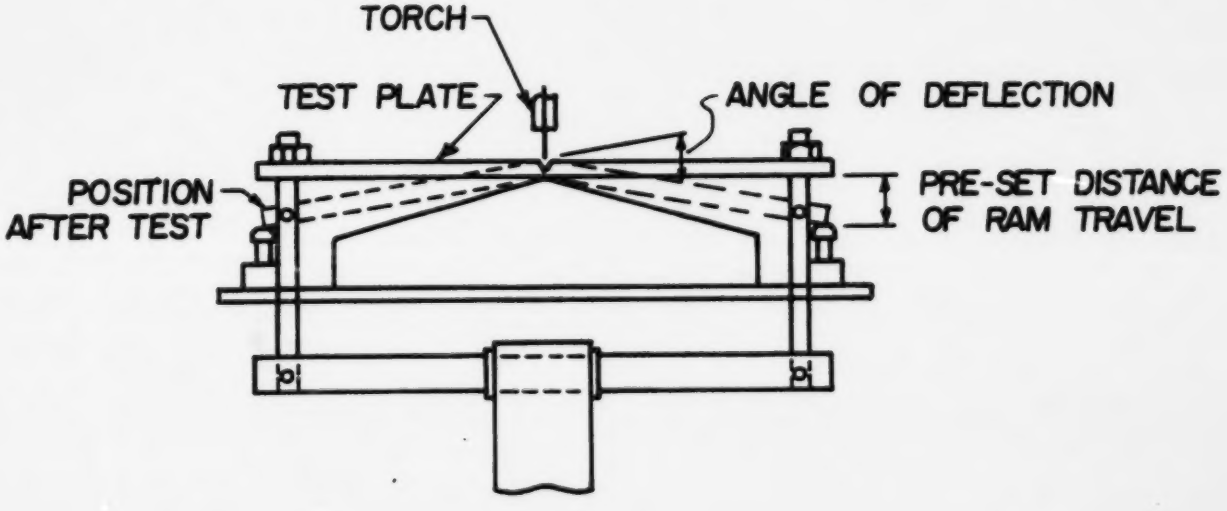

Figure 11. Principle of operation of Transvarestraint test.

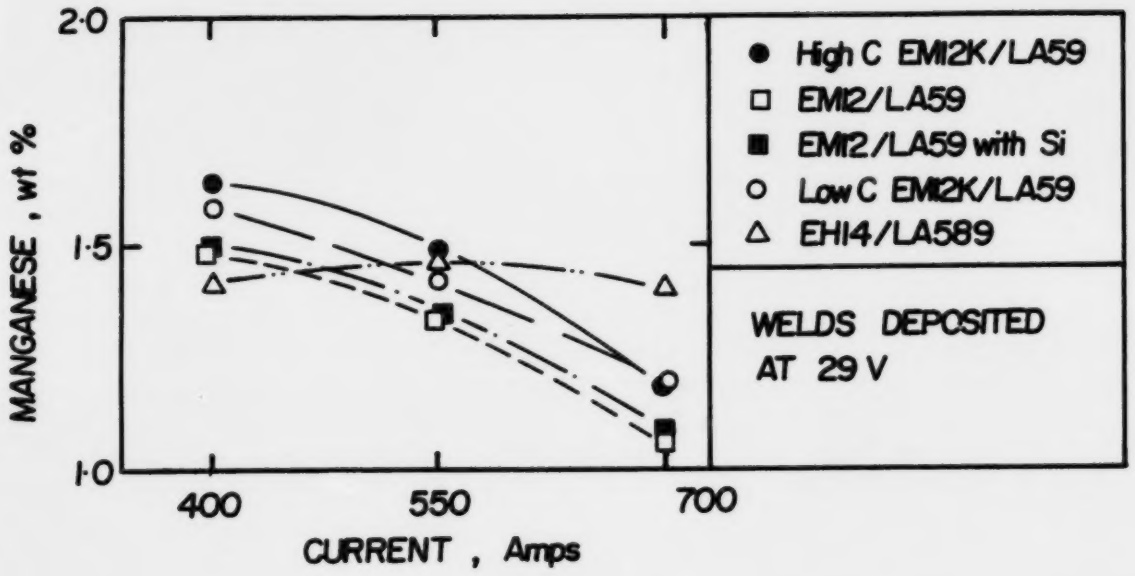

Figure 12. Variation in manganese content versus amperage for welds deposited at 29 V.

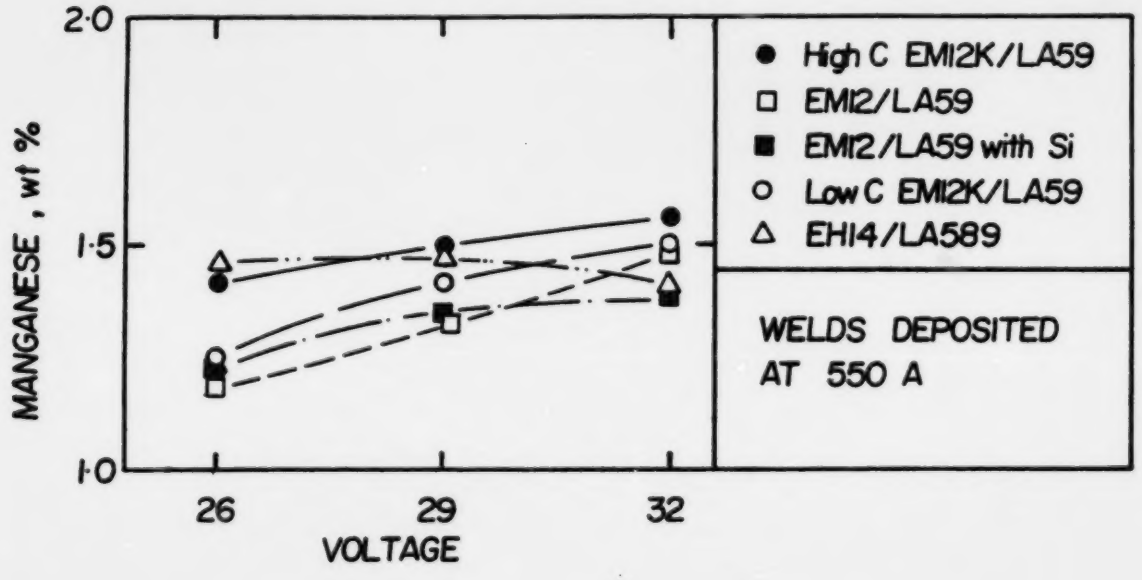

Figure 13. Variation in manganese content against arc voltage for welds deposited at 550 A.

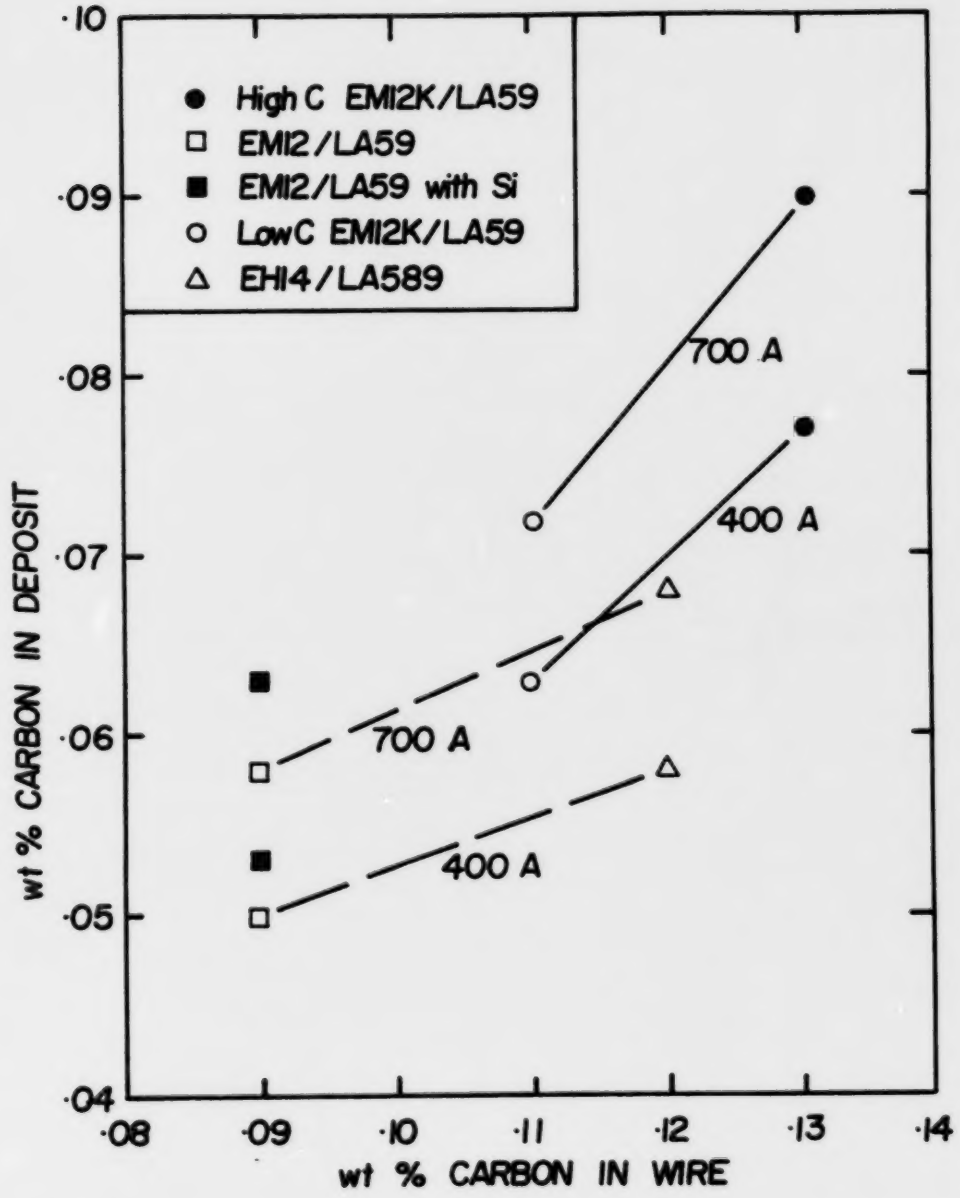

Figure 14. The influence of arc current on the transfer of carbon from the wire to the deposit.

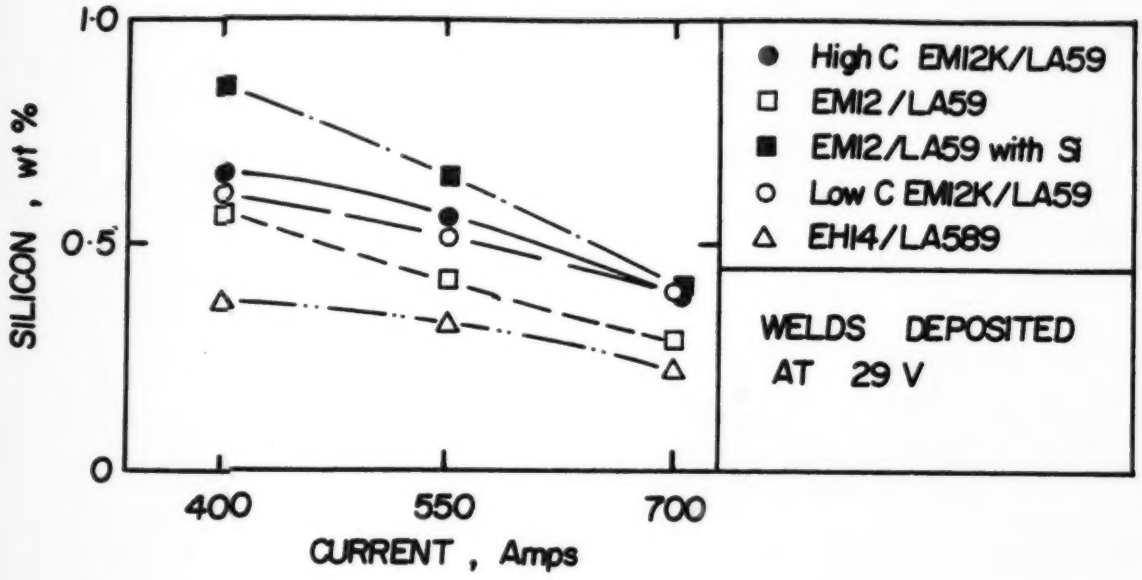

Figure 15. Variation in Si content versus current for welds deposited at 29 V.

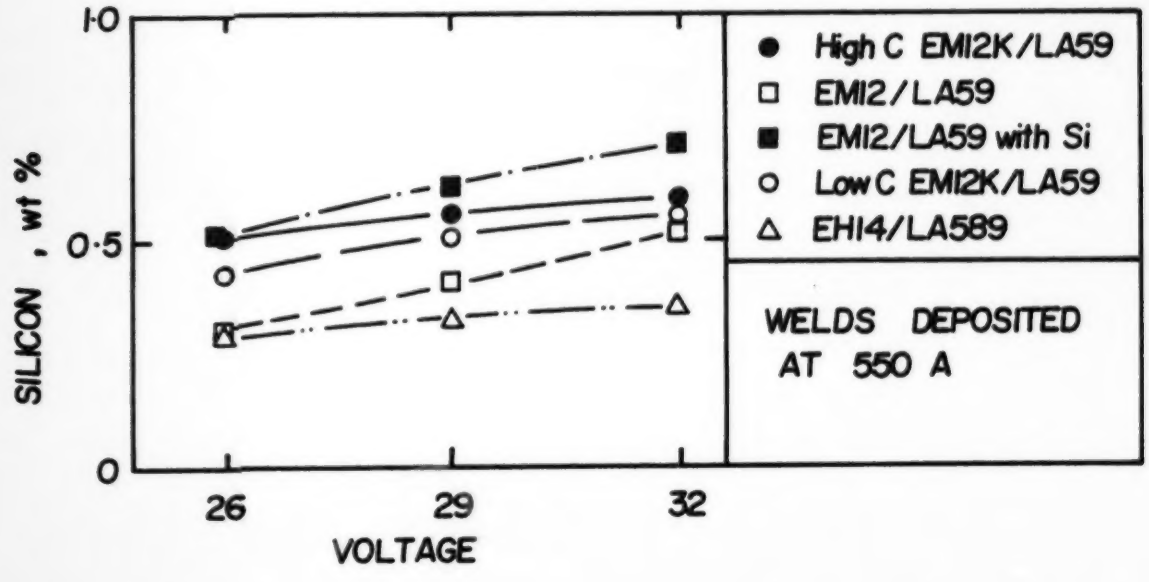

Figure 16. The influence of arc voltage on Si content for welds deposited at 550 A.

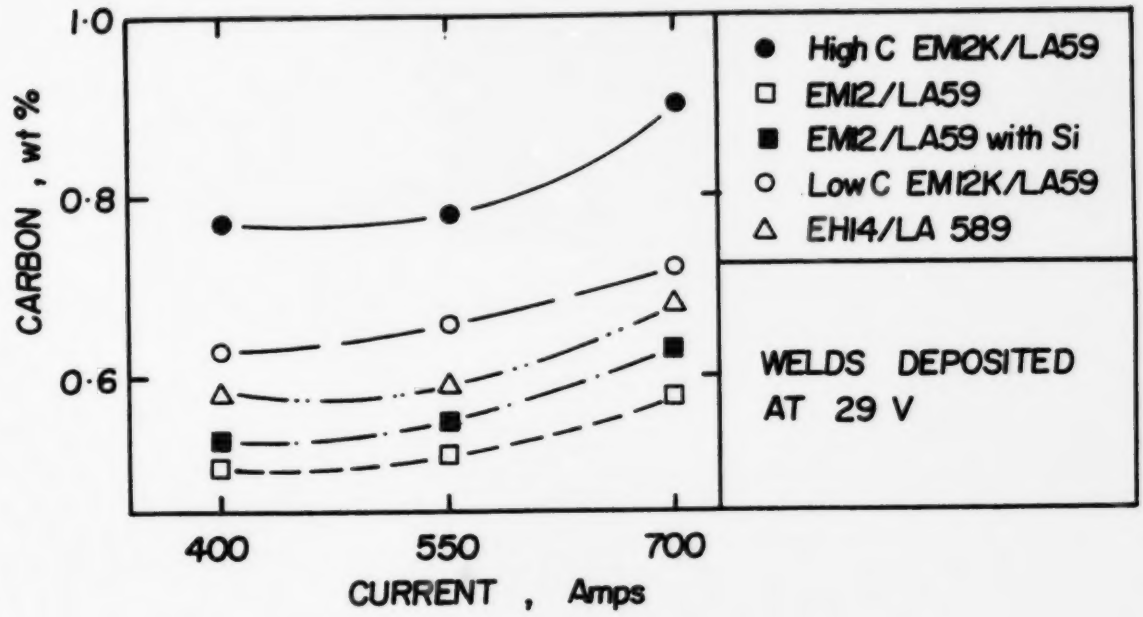

Figure 17. The influence of current on carbon content at an arc voltage of 29 V.

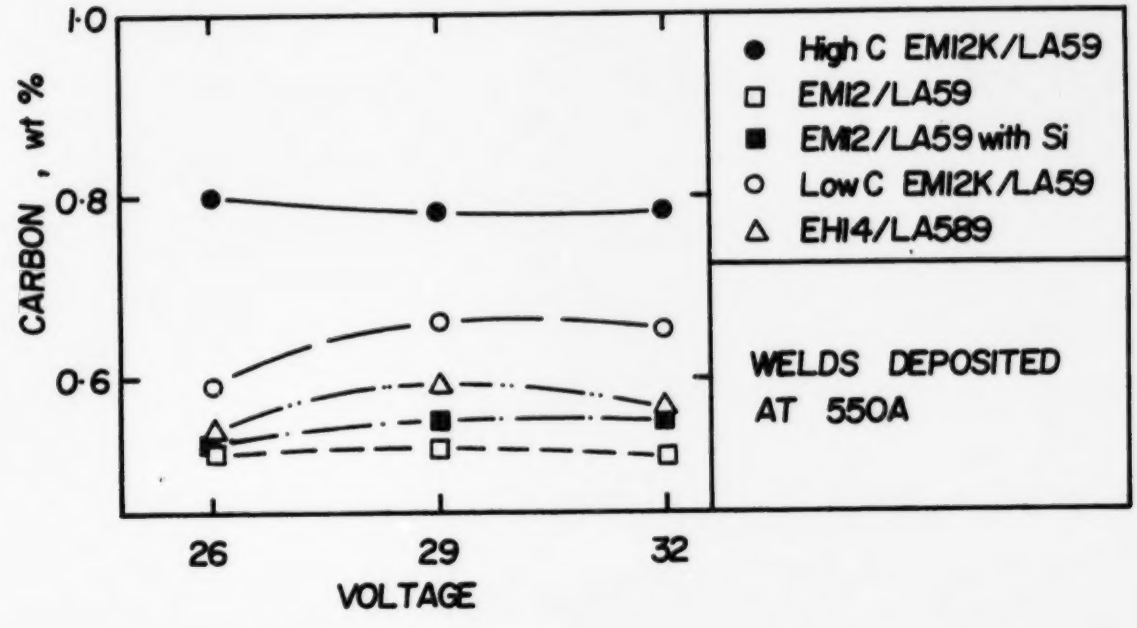

Figure 18. Variation in carbon content as a function of arc voltage for welds deposited at 550 A.

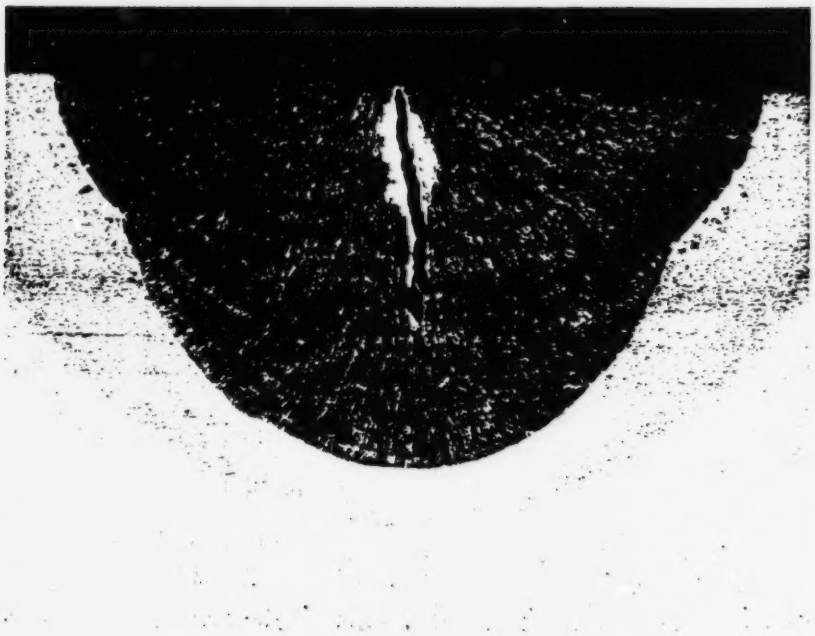

Figure 19. Typical example of solidification cracks observed on cross-section of Transvarestraint specimen, Neg 273C, X7 Mag.

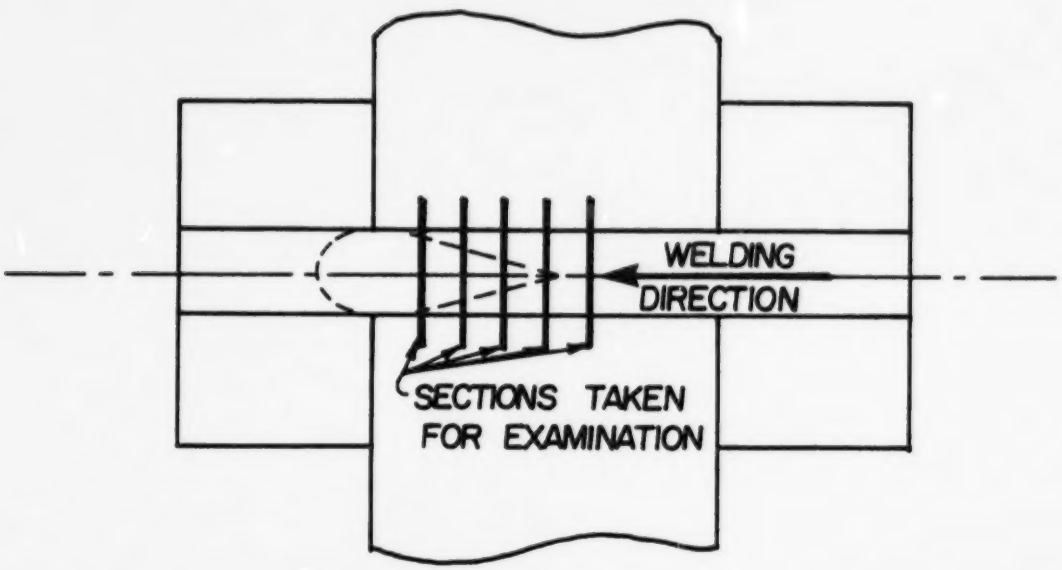

Figure 20. Detail of faces for examination of cracking in Transvarestraint tests.

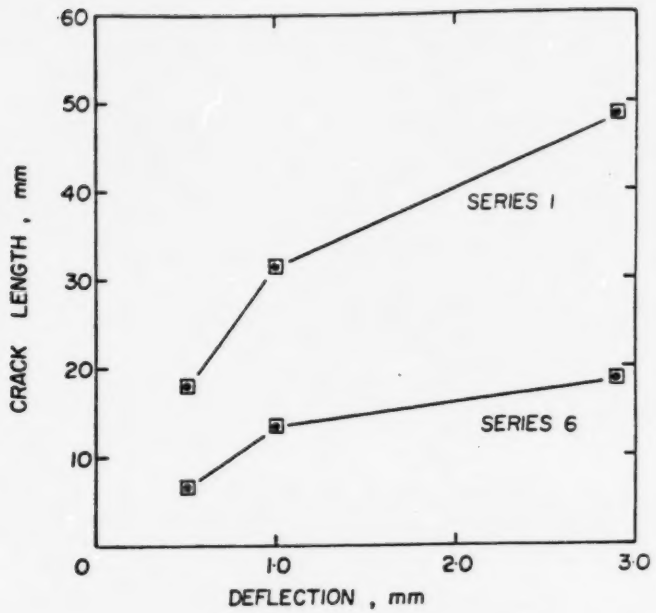

Figure 21. Crack severity versus deflection for series 1 and Series 6 welds, high C EM12K/LA59.

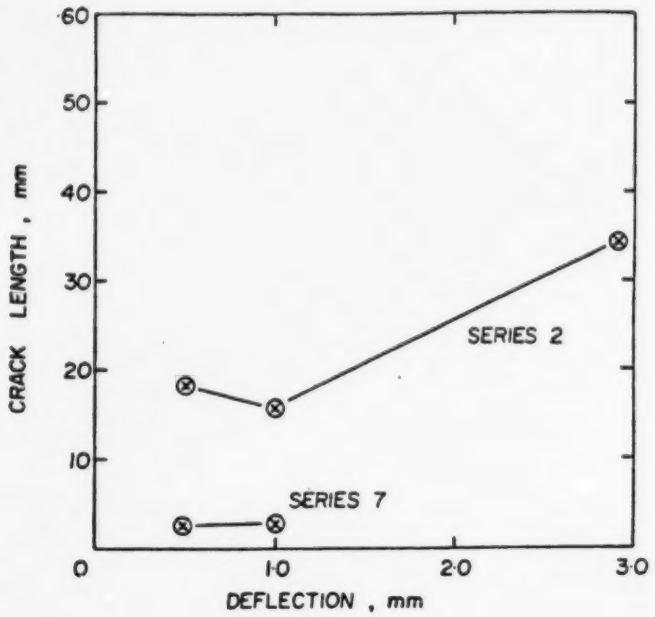

Figure 22. Crack severity versus deflection for Series 2 and Series 7 welds, EM12/LA59.

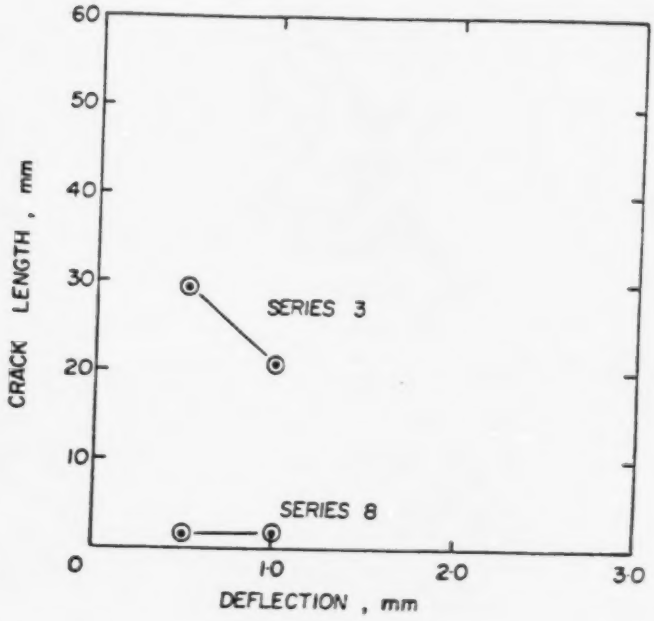

Figure 23. Crack severity versus deflection for Series 3 and Series 8 welds, EM12/LA59 with Si addition.

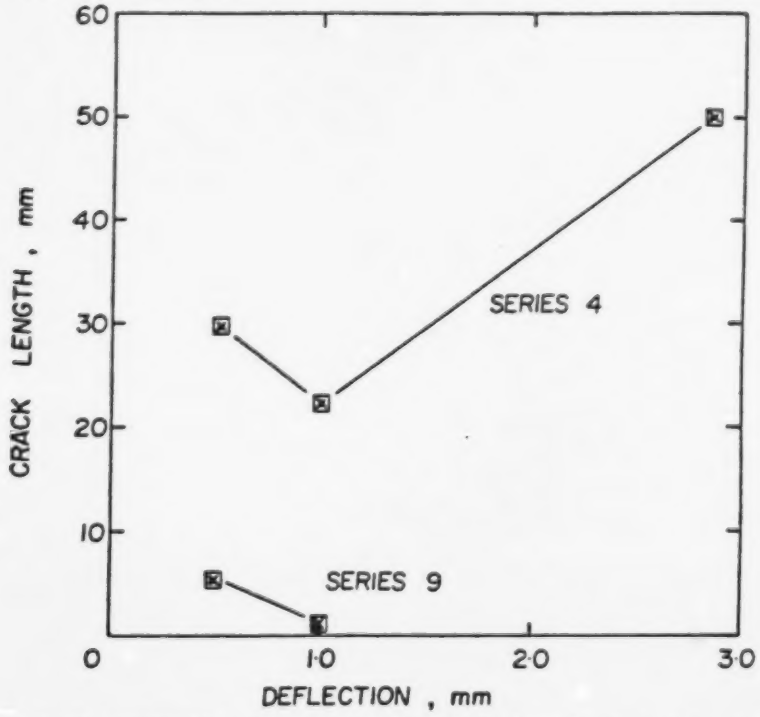

Figure 24. Crack severity versus deflection for Series 4 and Series 9 welds, low C EM12K/LA59.

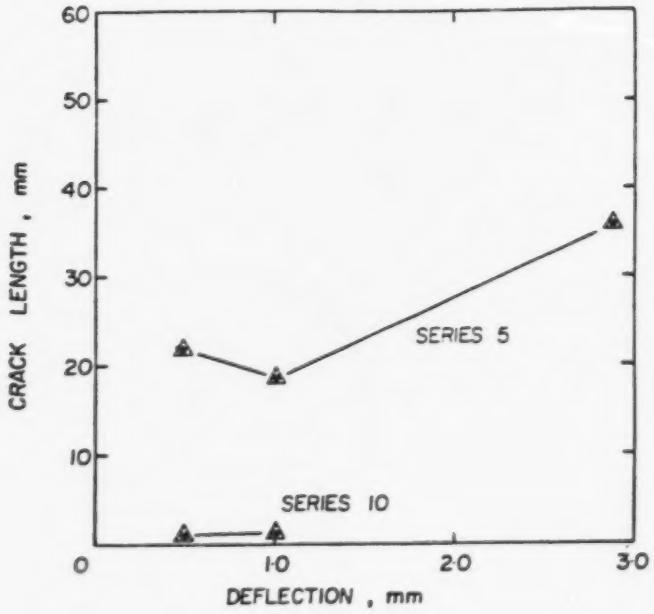

Figure 25. Crack severity versus deflection for Series 5 and Series 10 welds, EH14, 2% Mn/LA589.